

# Numerical (CFD) Analysis of Thermal Spray Coating Process

T. Raja jayasingh<sup>1</sup>, T. Raja jeyaseelan<sup>2</sup>, C. Kannan<sup>3</sup>, M. Ganesh Karthikeyan<sup>4</sup>  
<sup>1,3,4</sup> (Assistant Professors Mechanical Department, TRP Engineering College, Trichy, India)  
<sup>2</sup> (Assistant Professor Mechanical Department, the Rajas Engineering College Vadakkankulam)

**ABSTRACT:** numerical study of Thermal spraying process is required for optimizing performance and gun design for spraying various materials. Cold spray process is a new technique of thermal spray process which is used in industries and very limited data is available. This paper presents an investigation on the powder stream characteristics in cold spray supersonic nozzles. This work describes a detailed study of the various parameters, namely applied gas pressure, gas temperature, size of particles, outlet gas velocity, dimensions of the nozzle on the outlet velocity of the particles. A model of a two-dimensional axisymmetric nozzle was used to generate the flow field of particles (copper or tin) with the help of a carrier gas (compressed) stream like nitrogen or helium flowing at supersonic speed. Particles are dragged by the carrier gas up to high velocity magnitudes, resulting in severe plastic deformation processes upon impact with a solid substrate positioned at the distance SoD (Standoff Distance).

**Keywords:** Carrier gas, Cold spray, Critical velocity, Substrate, Stand-off distance, FLUENT.

## I. Introduction

Over the past few years new spraying techniques for coating purposes have been experimentally and computationally analyzed for better understanding of the thermo-mechanical processes involved. Cold spray technology is attracting the researchers and industries worldwide because of its advantages over the other spraying methods [1]. The cold spray dynamic technology is a new technique for coating metals with very small metal powder particles using compressed gas stream propulsion. This technology was developed with the aim of producing pore free and non oxidized coatings which were not possible with other conventional coating techniques like HVOF, Plasma spraying and arc spraying. Due to the high velocity of particles, this process gives a highly bonded coating with good adhesion between particles and substrate, low friction coefficient, high thermal and electrical conductivity, and excellent corrosion and oxidation resistance [2].

Many companies and researchers worldwide are working on cold spray. In USA, research on cold spray technology was first undertaken by a consortium formed under the auspices of the National Centre for Manufacturing Sciences (NCMS). After that many research centers became interested in this technology e.g. the Institute of Theoretical and Applied Mechanics of the Russian Academy of Science, Sandia National Laboratories and Pennsylvania State University [3]. Sandia National Lab had funded companies like ASB Industries, Ford, K-Tech, Pratt & Whitney to a value of 0.5 million U.S. dollars a year for 3 years to do R&D and develop this technology. Pennsylvania State University have received grants from the U.S. Navy to do R&D on the cold spray process and develop an anti skid coating [4].

### 1.1 Thermal Spraying

Thermal spray is the process in which a metal or alloy in molten or semi molten state is used to make a layer on a substrate. The thermal spray technique was first used in the early 1900s when Dr Schoop (refer to the Master patent of Schoop technology) [5] used a flame as a heat source. Initially it was practiced on metals with low melting point and after that it was progressively extended to metals with high melting point [5]. For making the deposit in thermal spraying a stream of molten metal particles strike a substrate, become flattened and then undergo rapid solidification and quenching. Every droplet spreads to make its own layer and these layers join to make a deposit of thermally sprayed material. In this process voids are formed in the deposit mainly because of incomplete filling or incomplete wetting of the molten metal and during the quenching of brittle materials micro cracks are formed after the solidification of molten material. These affect the mechanical properties like elastic modulus and stress at failure and physical properties like thermal conductivity [6].

### 1.1.1 Cold Spray Process

The phenomenon of cold spray was discovered during an aeronautical investigation in the 1980's. When dusty gases were used in shock tube experiments, the particles were observed to stick on the substrate. This process was undesirable but was recognized to be useful because particles of ductile metals or alloys could be bonded onto metal surfaces, glass or ceramics at impact velocities ranging from 400 to 1200 m/s. This is how coatings are made on work pieces [15]

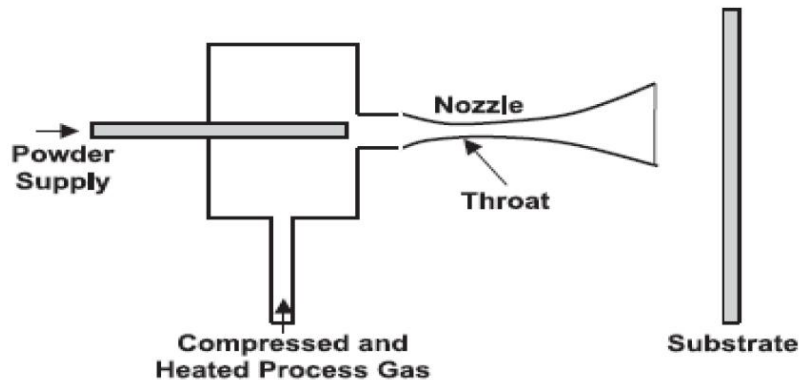


Figure 1.1: Schematic diagram of cold spraying system

The cold spray process or cold gas-dynamic process is a coating process utilizing high speed metal or alloy particles ranging from 1 to 50  $\mu\text{m}$  in size, with a supersonic jet of compressed gas with a velocity ranging from 300 to 1200 m/s on the surface of the work piece is shown in Fig.1.1. The coating formed by this process depends upon a combination of factors like particle velocity, temperature and size. The powder particles in this process are accelerated by a supersonic gas jet at a temperature lower than its melting point, thus reducing many effects which occur in high temperature spraying like oxidation at high temperature, melting of the substrate or spray particles, crystallization, evaporation, stress generation, gas release and other related problems [16].

Studies on cold spraying shows that the most important parameter is the velocity of the particles before they strike the substrate. For making a successful coating the particles should strike the substrate at a higher velocity than a critical velocity [17].

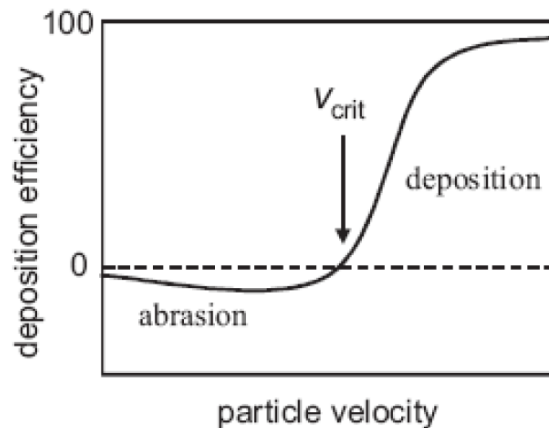


Figure 1.2: Correlation between the particle velocity and deposition efficiency

If the particles strike the substrate at a velocity lower than the critical velocity then the particles will just scratch the surface of the substrate as they do in grit blasting. By increasing the particle velocity the deposition efficiency reaches saturation point which is nearer to 100%. Most of the research related to cold spray is focused on achieving high particle velocity by making new designs of the nozzle used for spraying [17].

#### 1.1.1.1 Reason for Doing Cold Spraying

In the cold spray process, particles ranging in size from 5 to 50  $\mu\text{m}$  are used to make a coating by number of layers. The cold spray process is relatively better for making thicker coatings than thermal spraying because there are no thermal stresses involved in it [18]. A most important consideration in introducing new

process to industry is a reduction in the manufacturing cost of components. Most components in industry are fabricated by casting which is the initial step in the production line. The Pratt & Whitney Company as a part of the US Air Force forging supplier has developed a model called value stream analysis which shows that reduction in cost cannot be achieved by reducing the cost of one area in a production line. Pratt & Whitney also developed a model for Laser Powder Deposition of titanium and this model has been extended to model the cold spray process for titanium [4].

### 1.1.1.2 Equipment Used in Sprayin

A block diagram of cold spray equipment with a powder heater installed is shown in fig.1.3

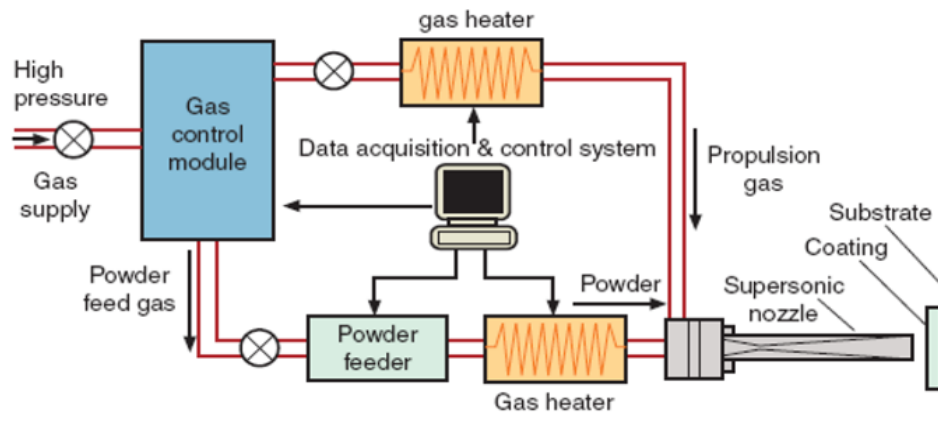


Figure 1.3: The block diagram of cold spraying system

The main parts of the cold spray system involves

- 1) A gas control module which contains the working gases such as helium, nitrogen, argon, and mixes of these gases and which enter the nozzle at higher pressure.
- 2) A data acquisition and control system for controlling the gas pressure from the compressor, the powder feed rate into the nozzle and the gas heater that maintains the proper temperature of the gas.[20]
- 3) A powder feeder which delivers powder in a continuous flow at a mass flow rate of 5 to 10 kg/h to make a uniform coating and improve reliability for measuring deposition efficiency. The powder feeders currently available with features like low maintenance, uniform and accurate powder feeding, low powder wastage, minimal pulsing and easy cleaning.[16]
- 4) A gas heater is used to heat the gas up to a temperature ranging from 300° to 650°C before it enters the nozzle. Heating the gas eventually increases the powder particles temperature and velocity and hence ensures plastic deformation after they strike a substrate. However the gas temperature at the inlet of the nozzle is below melting point which means particles do not melt during the process.[21]
- 5) In the coating process, nozzle is the main component for depositing solid-state particles. In the cold spray process, a convergent-divergent De Laval type nozzle is used to accelerate the particles at supersonic speed by the gas flow. After leaving the nozzle at high velocity, the particles impinge on the work piece and undergo plastic deformation because of collision and bonding with the work piece surface and other particles to make a coating. Studies show [22] that better injection through the nozzle gives the following benefits in coating formation:-
  - a) It enables the use of an increased gas temperature for the cold spray process.
  - b) The dwell time of the sprayed particles can be increased before they enter the convergent divergent nozzle and heat the particle.
  - c) More powder gas flow can be used without clogging the nozzle hence increasing the effective temperature of propellant gas [22].

### 1.1.1.3 Factors Affecting the Cold Spray Process

Recent research on the cold spray process shows that successful coating formation on a substrate depends upon the velocity of the particles exiting the nozzle and striking the surface of work piece. The velocity further depends upon factors such as gas temperature, gas pressure, type of gas used [23], the size of the particles used for spraying and the nozzle design which includes the throat diameter, inlet diameter, outlet diameter, convergent and divergent length of the nozzle [24].

### 1.1.1.3.1 Effect of Gas Temperature

Previous studies have found that if the temperature of the carrier gas is increased then it directly affects the velocity of the particles [21] [22] [25] and it also results in higher deposition efficiency of the particles on the substrate. Compressed gas enters the convergent divergent nozzle with an inlet pressure of around 27-35 bar to get the supersonic velocity. The solid powder particles are introduced in the nozzle upstream (convergent portion) and are accelerated by the rapidly expanding gas in the divergent part of the nozzle. The carrier gas is often preheated to get high gas flow velocities through the nozzle. In the cold spray process the gas is first heated to a temperature ranging from 300 K to 900 K. Particles when introduced into a hot gas stream, are in contact with the gas for a shorter time, so that when the gas expands in the divergent part its temperature decreases. In this process the temperature of the particles remains below their melting temperature [26]. The main gases which are used for cold spraying are helium and nitrogen because of their lower molecular weight and larger specific heat ratio.

The main consideration arising from increasing the temperature of the gas is the robustness of the nozzle material, which results in getting limited particle velocity and temperature. The German company CGT commercially manufactured a tungsten carbide MOC-nozzle which can spray copper particles at 600° C at a pressure of 30 bars without plugging and erosion of the nozzle material [25]. The main advantage of a high impact temperature is that it decreases the critical velocity of the spray material because of thermal softening. The deposition efficiency also depends upon the temperature of the carrier gas. It was found that when nitrogen is used to spray titanium particles the critical temperature is 155 °C, below this temperature no particle deposition took place. When the temperature was further increased from this critical temperature, the deposition efficiency also increased rapidly, especially when the temperature of nitrogen exceeded 215 °C.

### 1.1.1.3.2 Effect of Gas Pressure

In an experiment performed by M. Fukumoto *et al* [27] the effect of the gas inlet pressure on the deposition efficiency was investigated and the results showed that deposition efficiency increases with increase in the gas pressure.

Cold spray systems are subdivided into two categories high pressure systems and low pressure systems on the basis of gas pressure. Fig.1.4 shows the higher pressure system. A separate gas compressor is required in these systems and gases such as helium is used in this system because of its low molecular weight to achieve very high particle velocity. Fig.1.5 shows the lower pressure system. In a low pressure system a powder stream is injected into the nozzle at the point where gas has expanded to low pressure. Since no pressurized feeder is required in this system, it is often used in portable cold spray systems.

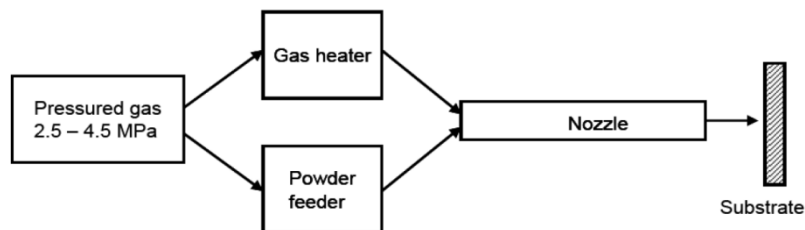


Figure 1.4: High pressure system

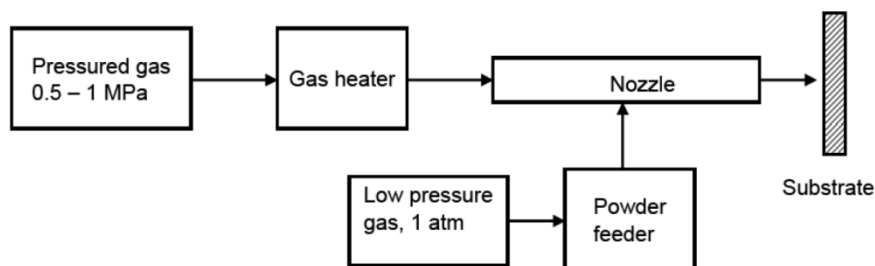


Figure 1.5: Low pressure system

### 1.1.1.3.3 The Effect of the Type of Gas

In cold spray processes the type of gas used to spray powder particles plays an important role in the acceleration of particles. In most cases nitrogen, helium, air or the mixture of air and helium or air and nitrogen are used as carrier gasses because of their lower molecular weight [28].

Initially experiments using helium as a carrier gas were very successful in achieving high adhesion and corrosion resistant coatings. Cold spray process parameters were also developed with nitrogen to reduce the costs while maintaining satisfactory coating performance [29]. In one-dimensional flow theory the Mach number at the throat is assumed to be unity and the velocity of gas can be calculated from:

$$V = \sqrt{\gamma RT}$$

Where  $\gamma$  is specific heat ratio, T is temperature of gas and R is the specific gas constant (the universal gas constant is divided by the gas molecular weight). The above equation shows why it is often found that helium makes a better carrier gas for cold spraying. It has a smaller molecular weight and higher specific heat ratio [23]. The specific heat ratios of nitrogen and helium are 1.4 and 1.66 respectively. The specific gas constants for nitrogen and helium are 296.8 J/Kg K and 2,077 J/Kg K respectively. According to the above equation the velocity of nitrogen will be lower than the velocity of helium, and when the temperature of the gas is increased the gas velocity increases. Subsequently the particle velocity also increases. The drag force on particles increases when gas pressure is increased because higher gas pressure increases the density of the gas [24].

**1.1.1.3.4 The Effect of Particle Size**

Previous study shows that the powder particles used for spraying have a wide size distribution range [28][29][30]. The powder is fed into a gas stream flowing through the nozzle. The acceleration of each particle depends upon its size. Particles cannot make a coating if they are very small in size or light in weight, because then they will follow the flow where as if the powder particles are very heavy or large in size they will not get the kinetic energy from the carrier gas to strike the substrate [30]. Small particles achieve high acceleration and large particles achieve less acceleration. For making a successful powder deposit only the particles with a velocity greater than a critical velocity can contribute to the coating. Hence it is very important to consider the particle size before carrying out cold spraying. The particles size distribution can be expressed by the following Rosin-Rammler formula:

$$Y_d = e^{-\left(\frac{d}{\bar{d}}\right)^n}$$

Where  $Y_d$  is the mass fraction and 'n' is the size distribution. At high temperatures more plastic deformation occurs in particles when they strike a substrate and this improves deposition efficiency [31]. A previous study shows that the particle temperature reaches maximum value when the diameter of the particle is 10µm. This behaviour is determined by the particle and gas phase heat transfer. There is a maximum temperature profile for the smaller particles because the heat transfer rate is faster for smaller particles. In larger particles, the temperature increases slowly [32].

**II. Numerical Methodology**

**2.1 Geometry**

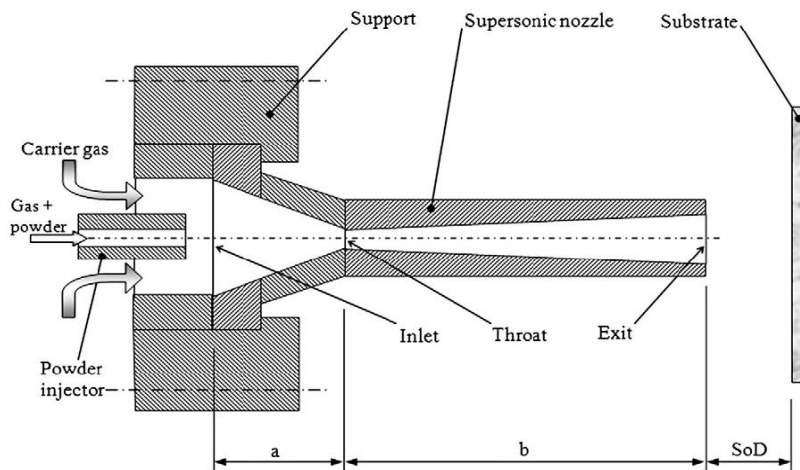


Figure 2.1: Schematic of the Nozzle

A schematic diagram of the cold spray system is shown in fig.2.1. The spraying gun of the system comprises a supersonic converging– diverging nozzle and a powder injector. The injector outlet is located near the convergent part of the nozzle because it is a high pressure system. In low pressure system the injector outlet is located after the throat( low pressure area ) of the nozzle. A pressurized carrier gas fed through a number of ports enters the nozzle inlet zone of length a. At the same time, a mixture of gas and powder is delivered from a powder feeder to the powder injector shown in the figure. The carrier gas will therefore expand up to atmospheric pressure and accelerate throughout the main nozzle total length (a+b), giving sonic velocity at the throat and supersonic velocity at the exit. Particles are dragged by the carrier gas up to high velocity magnitudes, resulting in severe plastic deformation processes upon impact with a solid substrate positioned at the distance SoD (Standoff Distance). As a consequence, bonding with the substrate can occur and the coating process can be initiated. The substrate is connected to a CNC table which moves the substrate inX and Y directions at an imposed speed.

## 2.1 Introduction to CFD

Euler-Lagrange (Two way coupling) Discrete Phase Modeling (DPM) algorithm implemented in Fluent 13 was used in this study. In this approach the fluid phase is treated as a continuum by solving the Navier-Stokes equations, while the dispersed phase is solved by tracking a large number of particles through the calculated flow field. The dispersed phase can exchange momentum, mass, and energy with the fluid phase. The physical properties of all fluid flow are governed by the following three fundamental equations:

The general continuity equation is written as follows:

$$\frac{\partial \rho}{\partial t} + \frac{\partial}{\partial x_i}(\rho u_i) = 0$$

Here  $\rho$  is the density

The momentum equation that is solved in this study is:

$$\frac{\partial}{\partial t}(\rho u_i) + \frac{\partial}{\partial x_j}(\rho u_i u_j) = -\frac{\partial p}{\partial x_i} + \frac{\partial \tau_{ij}}{\partial x_j} + \rho g_i + F_i$$

Where  $p$  is static pressure,  $\tau_{ij}$  is the stress tensor,  $\rho g_i$  is the body force due to gravity and  $F_i$  is the external body force. As we are dealing with supersonic flow,  $\rho g_i$  is very small compared to external body forces, so it is neglected in this study.

The energy equation is written as follows:

$$\frac{\partial}{\partial t}(\rho E) + \frac{\partial}{\partial x_i}(u_i(\rho E + P)) = \frac{\partial}{\partial x_i} \left[ k \frac{\partial T}{\partial x_i} - \sum_j h_j J_j + u_j \tau_{ij} \right] + S_h$$

Where  $E$  is the total energy per unit mass,  $k$  is the conductivity,  $J_j$  is the diffusion flux of species  $j$  and  $S_h$  is the source term which refers to any heat source.

These basic principles for a flowing fluid can be written mathematically in the form of partial differential equations. Basically Computational Fluid Dynamics (CFD) replaces the governing differential equations with numbers to represent the fluid flow, and these numbers are put in three-dimensional space with a time interval to get the desired flow field in numerical form. The final outcome of the CFD is a group of numbers in closed form which represent a flow field analytically. The application of CFD for more complex and sophisticated cases depends mostly upon the computational resources like storage capacity and computational speed (RAM) [40].

## 2.2 Introduction to Ansys FLUENT

AnsysFluent is one of the major commercially available computational fluid dynamics (CFD) software. For doing Computational Fluid Dynamics AnsysFLUENT uses computer as a tool for analyzing and designing models. Fluent is computer software used for making models of flowing fluid and heat transfer. In fluent geometry of very complex models can be formed by using different type of meshes for solving the problems related to fluid flow. It also allows the mesh refining or coarsening depends on the solution required [40].

## 2.3 Numerical Procedure

To attain supersonic velocity of the gas stream, it is necessary to construct the geometry of aConvergent-divergent de-Laval nozzle [41]. ICEM CFD is used to create the geometry and mesh used in this study. The simulation can be used to determine the various flow parameters like the pressure and temperature of

the gas phase, velocity of the copper particles used in this spray, etc. It can also be used to determine the optimum operating parameters needed for achieve a good quality cold spray. For analyzing the flow parameters, 3D model & 2D axisymmetric model of the nozzle was created, because 3D model will predict the turbulence accurately. The reasons for making axisymmetric were:

- It reduces the computational effort required to solve the problem, and therefore it takes less time to get a converged solution.
- Flow field and geometry were symmetrical.
- Zero normal velocity at the plane of symmetry.
- Zero normal gradients of all variables at plane of symmetry.

The plane of symmetry was specified as the axis in boundary specifications and the nozzle model was defined such that flow, pressure gradient and temperature were zero along this specified edge of the domain. Using an axisymmetric model reduces computational effort but it does not affect the outcome of the simulation. Y. Li *et al.* [42] who investigated both the axisymmetric nozzle and two-dimensional full nozzle, found good agreement with the experimental results.

### 2.3.1 Model Parameters

The nozzle for cold spraying of copper particles was simulated by commercial code AnsysFLUENT 13 using the 2D double precision density solver to see the effects of the different parameters on the velocity of the copper particles, and how changing different parameters like temperature, pressure and size of the particles affects their velocity. From the literature[42], it was found that the velocity of the particles could be influenced by the nozzle expansion ratio (i.e. ratio of area of exit of nozzle to the area of throat). The coupled implicit density-based solver along with the Green-Gauss Cell Based gradient method was used to simulate the flow field inside the nozzle. The flow, turbulent kinetic energy, and turbulent dissipation rate were modelled using second order upwind accuracy.

### 2.3.2 Second Order Scheme

In the second order scheme, the values of cells are computed by using a multidimensional linear reconstruction approach. This approach was used for obtaining higher order accuracy and is achieved at cell faces by a Taylor series expansion of the cell centred solution of the cell centroid. The face value  $\phi_f$  is computed using the following expression:

$$\phi_f = \phi + \nabla\phi \cdot \Delta s$$

Where  $\phi$  and  $\nabla\phi$  are the cell centred values and their gradient in the upstream cell, and  $\Delta s$  is the displacement vector from the upstream cell centroid to the face centroid. This formulation requires the determination of the gradient  $\nabla\phi$  in each cell. This gradient is computed by using the divergence theorem, which in discrete form is written as:

$$\Delta\phi = \frac{1}{V} \sum_f^{N_{faces}} \phi_f A$$

Here the face values  $\phi_f$  are computed by averaging  $\phi$  from the two cells adjacent to the face. Finally, the gradient  $\nabla\phi$  is limited so that no new maxima or minima are introduced.

## 2.4 Turbulence Modelling

The fluid flowing through the nozzle had a very high Reynolds number (more than 50,000), so the flow can be said to be fully turbulent. Different turbulence models adopt different approaches for tackling turbulence but choosing the right model ensures the accuracy of the final solution. Modelling turbulence is very complex and a highly technical field, and the selection of a turbulence model depends on factors including accuracy, computational time, resources available, and application. In this work Realizable k- $\epsilon$  turbulence model is used.

### 2.4.1 Realizable k- $\epsilon$ Turbulence Model

The realizable k- $\epsilon$  model is a relatively recent development and differs from the standard k- $\epsilon$  model in two important ways:

- The realizable k- $\epsilon$  model contains a new formulation for the turbulent viscosity.
- A new transport equation for the dissipation rate,  $\epsilon$  has been derived from an exact equation for the transport of the mean-square vorticity fluctuation.

The term “realizable” means that the model satisfies certain mathematical constraints on the Reynolds stresses, consistent with the physics of turbulent flows. The standard k- $\epsilon$  model or its variants like the RNG k- $\epsilon$  are realizable. An immediate benefit of the realizable k- $\epsilon$  model is that it more accurately predicts the

spreading rate of both planar and round jets. It is also likely to provide superior performance for flows involving rotation, boundary layers under strong adverse pressure gradients, separation, and recirculation. To understand the mathematics behind the realizable k-ε model, consider combining the Boussinesq relationship and the eddy viscosity definition to obtain the following expression for the normal Reynolds stress in an incompressible strained mean flow:

$$\overline{u^2} = \frac{2}{3}k - 2\vartheta_t \frac{\partial U}{\partial x}$$

Using  $\vartheta_t \equiv \frac{\mu_t}{\rho}$  one obtains the result that the normal stress,  $\overline{u^2}$ , which by definition is a positive quantity, becomes negative, i.e., “non-realizable”, when the strain is large enough to satisfy

$$\frac{k}{\varepsilon} \frac{\partial U}{\partial x} > \frac{1}{3C_\mu} \approx 3.7$$

Both the realizable and RNG k-ε models have shown substantial improvements over the standard k-ε model where the flow features include strong streamline curvature, vortices, and rotation. Studies have shown that the realizable model provides superior performance compared to other variants of k-ε model for separated flows and flows with complex secondary flow features. One of the weaknesses of the standard k-ε model or other traditional k-ε models lies with the modeled equation for the dissipation rate (ε). The well-known round-jet anomaly is considered to be mainly due to the modeled dissipation equation. The realizable k-ε was intended to address these deficiencies of traditional k-ε models by adopting the following:

- Eddy-viscosity formula involving a variable  $C_\mu$  originally proposed by Reynolds.
- dissipation(ε) is modelled based on the dynamic equation of the mean-square vorticity fluctuation.

## 2.5 Discrete Phase Modelling

AnsysFluent provides a model that is specially developed for spray simulations, or more general suspended particle trajectory simulations. This is the Discrete Phase Model (DPM) and it is based on the so-called Euler-Lagrange method. In the computational domain there are two separate phases present, namely the continuous and the discrete phase (particles). The transport equations from the previous section are solved for the continuous phase only and the motion of particles is dealt with particle trajectory calculations. Through an iterative solution procedure the mass, momentum and energy interaction between both phases can be realized. Some important aspects of the DPM model are presented in this section.

### 2.5.1 The Euler- Lagrange Approach

The discrete phase modelling follows the Euler-Lagrange approach. In this approach the fluid phase is treated as a continuum by solving the Navier-Stokes equations, while the dispersed phase is solved by tracking a large number of particles through the calculated flow field. The dispersed phase can exchange momentum, mass, and energy with the fluid phase. A fundamental assumption made in this model is that the dispersed second phase occupies a low volume fraction, even though high mass loading ( $\dot{m}_{particles} \geq \dot{m}_{fluid}$ ) is acceptable. The particle or droplet trajectories are computed individually at specified intervals during the fluid phase calculation. This makes the model appropriate for the modeling of spray dryers, coal and liquid fuel combustion, and some particle-laden flows.

### 2.5.2 Particle Motion

The trajectory calculation of a discrete phase particle is done by integrating the force balance on the particle, which is written in a Lagrangian reference frame. This force balance equates the particle inertia with the forces acting on the particle, and can be written (for the x direction in Cartesian coordinates) as

$$\frac{du_p}{dt} = F_D(u - u_p) + \frac{g_x(\rho_p - \rho)}{\rho_p} + F_x$$

where the left hand term is the acceleration of the particle,  $F_x$  is an additional acceleration due to external force field and the term with  $F_D$  is the drag force on the particle.  $F_D$  is defined as:

$$F_D = \frac{18\mu C_D R_e}{\rho_p d_p^2 24}$$

where  $u$  is the fluid phase velocity,  $u_p$  is the particle velocity,  $\mu$  is the molecular viscosity of the fluid,  $\rho$  is the fluid density,  $\rho_p$  is the density of the particle,  $d_p$  is the particle diameter and  $R_e$  is the relative Reynolds number.



### **2.5.3 Turbulent Dispersion of Particles**

The dispersion of particles due to turbulence in the fluid phase can be predicted using the stochastic tracking model or the particle cloud model. The stochastic tracking (random walk) model includes the effect of instantaneous turbulent velocity fluctuations on the particle trajectories through the use of stochastic methods. The particle cloud model tracks the statistical evolution of a cloud of particles about a mean trajectory. The concentration of particles within the cloud is represented by a Gaussian probability density function (PDF) about the mean trajectory. For stochastic tracking a model is available to account for the generation or dissipation of turbulence in the continuous phase. Turbulent dispersion of particles cannot be included if the Spalart-Allmaras turbulence model is used.

#### **2.5.3.1 Stochastic Tracking**

When the flow is turbulent, AnsysFLUENT will predict the trajectories of particles using the mean fluid phase velocity,  $\bar{u}$ , and the fluctuating velocity  $u'$

$$u = \bar{u} + u'$$

In the stochastic tracking approach, AnsysFLUENT predicts the turbulent dispersion of particles by integrating the trajectory equations for individual particles, using the instantaneous fluid velocity,  $\bar{u} + u'(t)$ , along the particle path during the integration. By computing the trajectory in this manner for a sufficient number of representative particles (termed the “number of tries”), the random effects of turbulence on the particle dispersion can be included. ANSYS FLUENT uses a stochastic method (random walk model) to determine the instantaneous gas velocity. In the discrete random walk (DRW) model, the fluctuating velocity components are discrete piecewise constant functions of time. Their random value is kept constant over an interval of time given by the characteristic lifetime of the eddies.

The DRW model may give nonphysical results in strongly nonhomogeneous diffusion-dominated flows, where small particles should become uniformly distributed. Instead, the DRW will show a tendency for such particles to concentrate in low-turbulence regions of the flow.

#### **2.5.3.2 Particle Cloud Tracking**

In particle cloud tracking, the turbulent dispersion of particles about a mean trajectory is calculated using statistical methods. The concentration of particles about the mean trajectory is represented by a Gaussian probability density function (PDF) whose variance is based on the degree of particle dispersion due to turbulent fluctuations. The mean trajectory is obtained by solving the ensemble-averaged equations of motion for all particles represented by the cloud. The cloud enters the domain either as a point source or with an initial diameter. The cloud expands due to turbulent dispersion as it is transported through the domain until it exits. As mentioned before, the distribution of particles in the cloud is defined by a probability density function (PDF) based on the position in the cloud relative to the cloud center. The value of the PDF represents the probability of finding particles represented by that cloud with residence time  $t$ .

### **2.5.4 Phase Coupling**

While the discrete particle phase is always influenced by the continuous phase solution (one-way coupling). However, when the particle influences the flow characteristics of the continuous phase, then it is called two way coupling. In the one-way coupling case the continuous phase is solved first thereafter the particle trajectory calculation is performed. When two-way coupling is applied an iterative procedure is followed. Then, after the particle trajectory calculation the continuous flow field is solved again with updated source terms until convergence is reached.

### **2.5.5 Discrete Phase Boundary Conditions**

The copper particles of varying sizes were used in the simulation to see their effect on the outlet velocity. The varying sizes of copper particles were used with an initial velocity of 30 m/s and an initial temperature of 300 K. The powder mass flow rate used for particle tracking was 10-15% less than the gas mass flow rate so that it would not disturb the gas flow field.

The following assumptions were made for DPM:

- 1) The copper particles were spherical in shape.
- 2) The particles introduced in the axial direction of the nozzle.
- 3) The particles were accelerated by the drag force of the gas used.
- 4) The temperature inside the copper particle was uniform.

For powder size distribution Rosin-Rammler diameter distribution method is used. If the size distribution is of the Rosin-Rammler type, the mass fraction of particles of diameter greater than  $d$  is given by:

$$Y_d = e^{-\left(\frac{d}{\bar{d}}\right)^n}$$

Where 'n' is the size distribution parameter and  $\bar{d}$  is the mean diameter of a particle.

### III. Results and Discussions

#### 3.1 Geometry

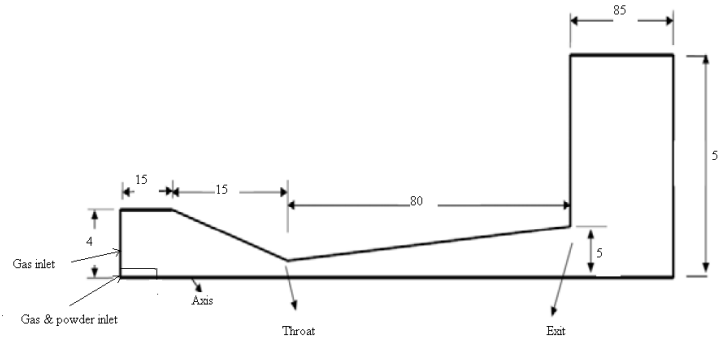


Figure 3.1: Geometry used for simulation

The 3.1 shows the dimensions of cold spray nozzle used for the simulation. The main aim of selecting this convergent-divergent nozzle is to attain the supersonic velocity of gas in the exit. A high pressure gas is preheated and led into a converging-diverging nozzle through the gas inlet. The cold spray copper powder is fed axially and centrally into the nozzle. In the divergent section, gas and powder particles are accelerated to supersonic velocity.

#### 3.2 Meshing

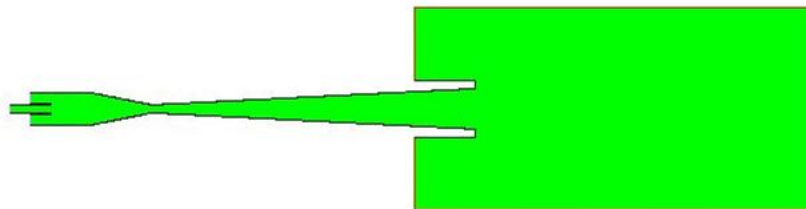


Figure 3.2: Computational Domain of Spray Gun created in ICEM-CFD

Meshing is the first and foremost step for the simulation process. It includes finding the dimensions for the sprat gun and discretizing the domain into finite volume cells. Meshing has significant impact on rate of convergence, solution accuracy and CPU time.

##### 3.2.1 Meshing Procedure

Modelling has been done with the above dimensions and used the meshing tool of AnsysICEM CFD. After meshing the mesh was subjected to a quality testing and following results were obtained.

Mesh quality : 0.9784 ( it ranges from 0 to 1, close to zero as low quality)  
 Maximum aspect ratio : 3.858  
 Number of cells : 54000 ( after analyzing mesh independence)

##### 3.3 Boundary Conditions for Base Case

Carrier Gas inlet : Pressure inlet  
 Gas & powder inlet : Pressure inlet  
 Gas outlet : pressure outlet  
 Carrier Gas inlet pressure : 21 bar  
 Outlet pressure : atmospheric pressure  
 Carrier gas inlet temperature : 473 K  
 Type of carrier gas used : Helium  
 Injector & nozzle wall : Adiabatic  
 Spray gun material : Steel

Particle injection type : Surface injection  
 Particle inlet temperature : 300 K  
 Particle velocity at inlet : 30m/s  
 Particle type : Inert  
 Particle Material : Copper  
 Diameter distribution : Rosin-Rammler

### 3.5 Validation

It is important to validate the computational values before implementing them into the practical work and assessing their usefulness. Validation was performed by comparing the present CFD results with previously published experimental [43] results. Different applications require a different degree of accuracy in the It is important to validate the computational values before implementing them into the practical work and assessing their usefulness. Validation was performed by comparing the present CFD results with previously published experimental [43] results. Different applications require a different degree of accuracy in the validation, so the validation process is flexible to allow for different degree of accuracy.

### 3.6 Velocity & Pressure Contours (Base Case)

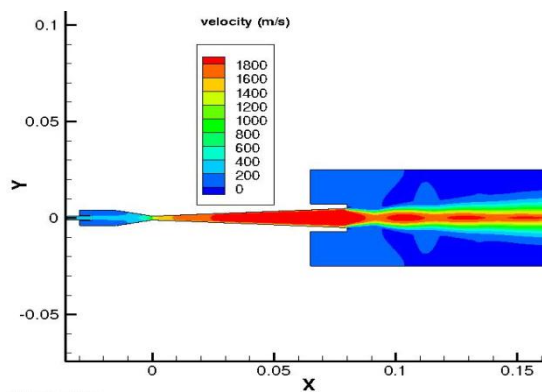


Figure 3.3: Velocity contour plot using helium as a carrier gas

Fig.3.3 shows contour plot of velocity magnitude between the inlet and outlet regions. The injection port pressure was set to 31.69 bar, to generate a mass flow rate of approximately 20% of the main gas (carrier gas inlet) flow. This condition falls within the optimum range for the current Cold Spray system to generate a consistent powder flow from the feeder. The gas phase maximum velocity is 1800 m/s, which corresponds to a Mach number of 3.5. The nozzle is shown to be over-expanded and therefore oblique shock waves develop at the exit.

Fig.3.4 shows the changes in pressure along the length of the nozzle. The pressure of the gas is high till the throat of the nozzle, After that the gas starts expanding in the divergent part of the nozzle and therefore the pressure decreases. At the exit of the nozzle the gauge pressure becomes nearly zero, Due to over expansion of the gas phase at the nozzle exit, Shock waves are formed and therefore pressure fluctuations are seen. The changes in pressure and velocity due to shock waves are clearly shown in fig.3.6. Several oblique shock waves are seen after the exit of the convergent- divergent nozzle due to the expansion of the supersonic gas as seen in fig.3.5.

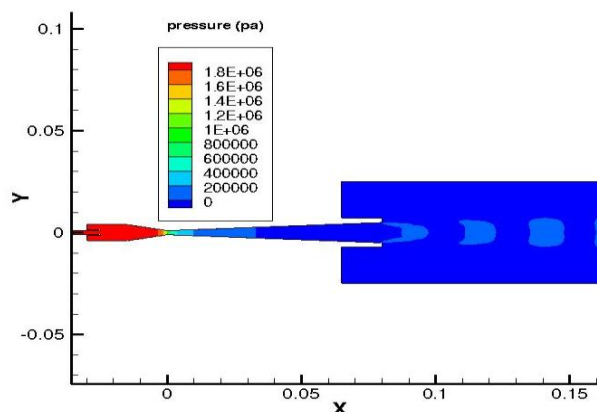


Figure 3.4: pressure contours

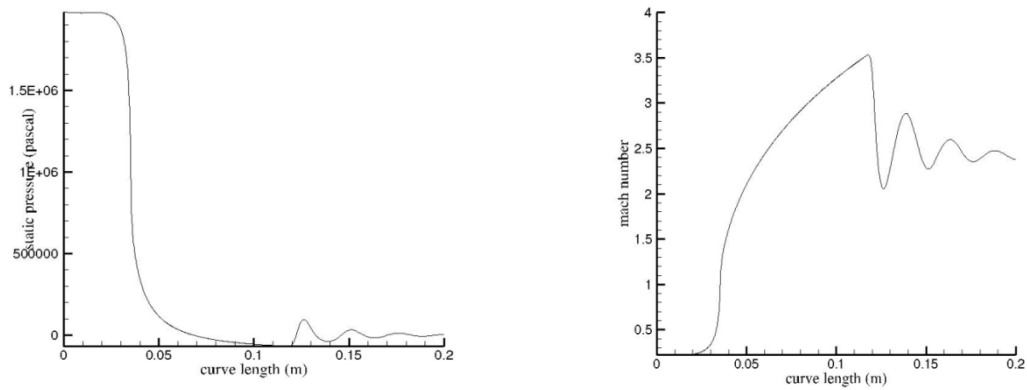


Figure 3.5: Profile of static pressure and Mach number distribution along the nozzle axis

### 3.7 Effects Various Carrier Gases on Particle Velocity

In this case only changing the type of gas used for the simulation and keep all other conditions are same as in the base case. Three types of gases were used in the simulation to see their effect on the velocity on copper particles through the nozzle.

The three different gases used for the simulation are helium, nitrogen and argon. Out of three gases, helium is the lightest gas because its molecular weight is lowest compared to the other two gases. The molecular weight of helium, nitrogen and argon are 4, 28 and 39.948 respectively. Because of the lower molecular weight, helium gas attains almost three times the velocity of nitrogen and argon at the exit of the spray gun is shown in fig.3.6.

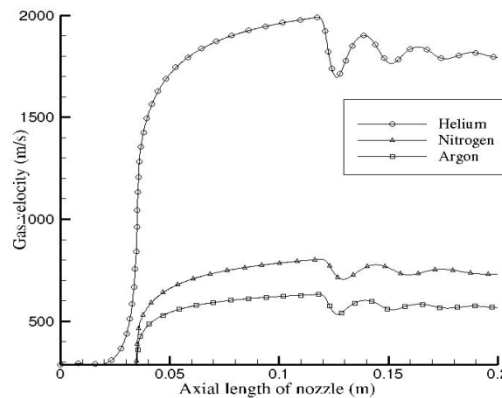


Figure 3.6: Velocity Variation of three Different Gases

Figs 3.7-3.9 shows the velocity profile along the axial length for different particle sizes when helium, nitrogen and argon are used as carrier gas. When helium is used it imparts the highest particle velocity compared to nitrogen and argon. It can be seen that there is an increase in particle velocity upto 200 m/s in the case of helium as compared to nitrogen.

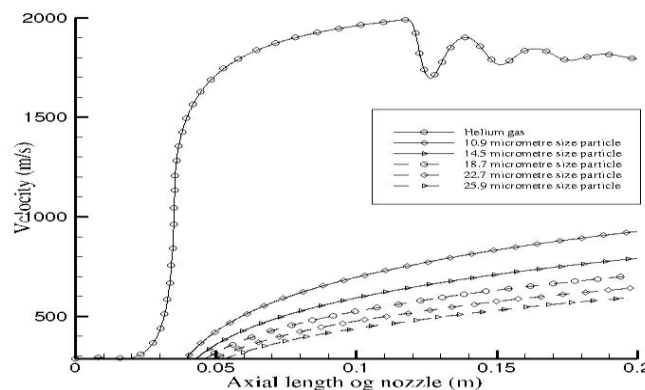


Figure 3.7: Velocity Variation of Particles by Using Helium as a Carrier Gas

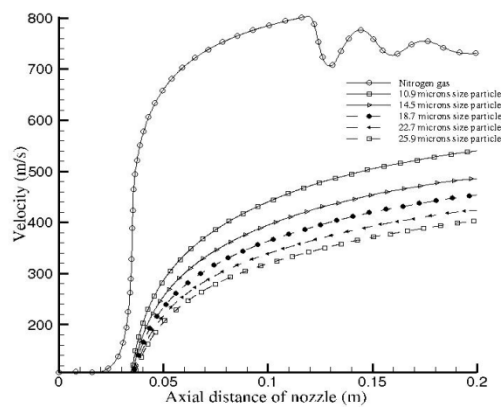


Figure 3.8: Velocity Variation of Particles by Using Nitrogen as a Carrier Gas

The Figs 3.7-3.9 shows that the particles reach approximately 42% of the gas velocity when helium is used, 60% of gas velocity when nitrogen is used and 70% when argon is used. Since the drag imparted to the particle improves with increasing molecular weight of the carrier gas, however, particles in helium has the highest velocity as the carrier gas has the highest velocity. Because of higher particle velocity by using by using helium results in a deposition efficiency of 75% as compared to 30 to 35% when using nitrogen or argon as a carrier gas.

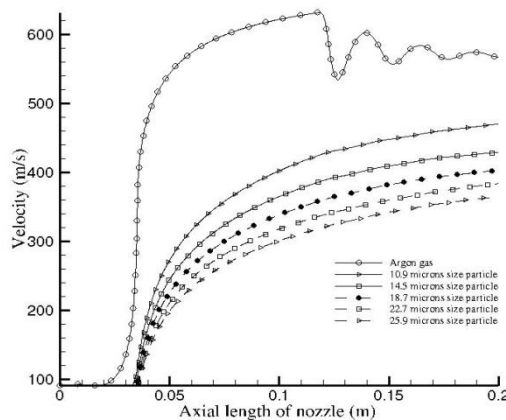


Figure 3.9: Velocity Variation of Particles by Using Argon as a carrier Gas

Fig.3.10 shows the mean particle velocity by using various carrier gases. In that curve clearly shows the particles achieve very high velocity by using helium as a carrier gas as compared to nitrogen and argon. The figs 3.7-3.9 Show that the particles of different sizes have different velocities. Velocities of the particles decrease with increase in particle size because acceleration due to drag on the particles depends on mass of the particles. So the lighter particles travel with higher velocity as compared to heavier particles.

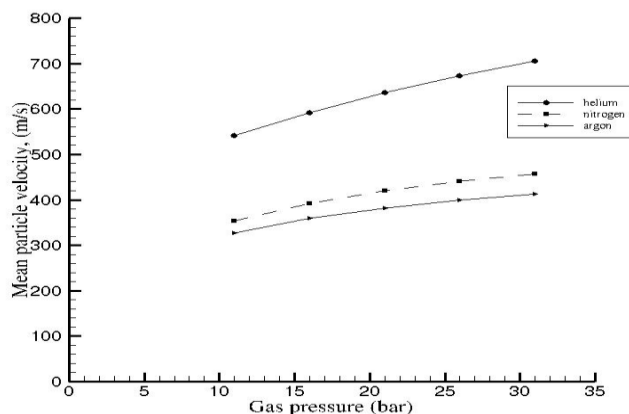


Figure 3.10: Effect of Carrier Gases on Mean Particle Velocity

### 3.8 Effect of Gas Temperature on Particle Velocity

In this case only changing the temperature of gas used for the simulation and keep all other conditions are same as in the base case.

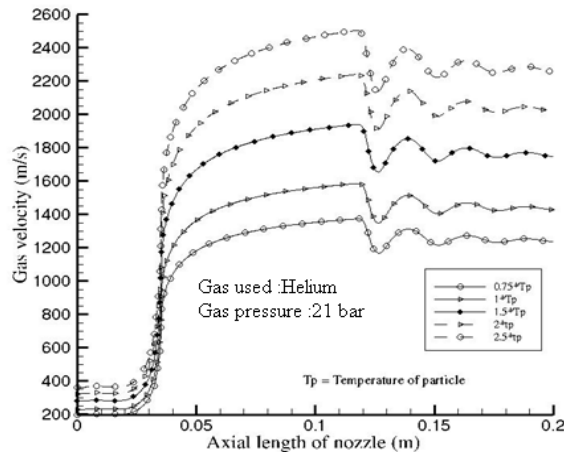


Figure 3.11: Effect of Gas Temperature on Gas Velocity

The deposition efficiency of particles depends upon the temperature of the carrier gas. It was reported earlier [25] that when nitrogen is used to spray titanium particles the critical temperature is 155 °C, below this temperature no particle deposition took place. When the temperature was further increased, the deposition efficiency also increased rapidly, especially when the temperature of nitrogen exceeded 215 °C. The reason behind the above statement is the critical velocity is a function of the temperature of carrier gas. Fig.3.11 shows the increase in carrier gas velocity by changing the carrier gas temperature. As the temperature of carrier gas is increased the velocity of particles also increase and it should result in higher deposition efficiency of the particles on the substrate.

Fig3.12 shows the variation in particle velocity at the outlet with varying gas temperature. As discussed earlier, switching from a carrier gas with higher molecular weight to one with lower molecular weight like helium results in increase in the mean particle velocity. In the same manner increase in gas inlet temperature results in decrease in gas density, therefore the overall drag on the particles increases.

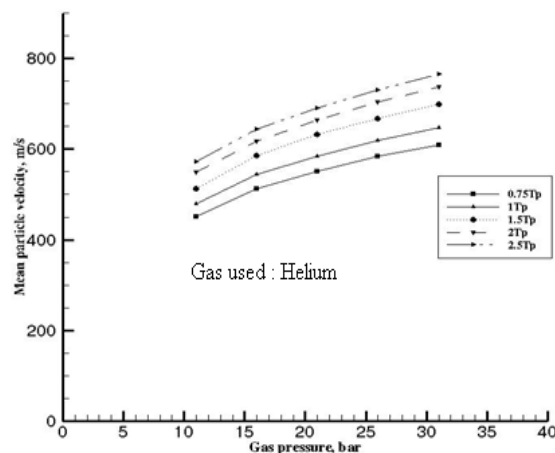


Figure 3.12: Effect of Carrier Gas Temperature on Mean Particle Velocity

### 3.9 Effect of Gas Pressure on Mean Particle Velocity

In this case only changing the inlet pressure of carrier gas used for the simulation and keep all other conditions are same as in the base case. The fig 3.13 shows the effect of changing the inlet pressure of carrier gas used for simulation. The variation in outlet gas velocity by changing the inlet carrier gas pressure is less as compared to changing carrier gas inlet temperature. But the particle velocity in the outlet increases, because increasing the inlet carrier gas increase the density of gas, so the drag on the particle increases.

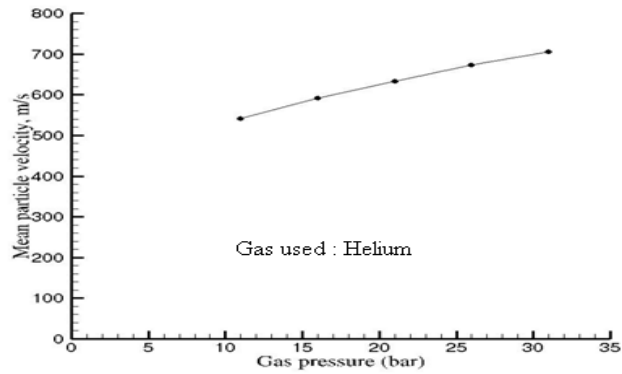


Figure 3.13: Effect Gas Pressure on Mean Particle Velocity

### 3.10 Effect of Particle Size on Mean Particle Velocity

The Rosin-Rammler distribution function is used for calculating the size distribution of particles. In Rosin-Rammler distribution the parameter ‘n’ called the spread parameter, by changing this parameter ‘n’ and finding various size distributions. If the parameter ‘n’ is increased, it will increase the difference between the diameter range of particles, and if the parameter ‘n’ is decreased the difference is increased is shown in fig.3.14

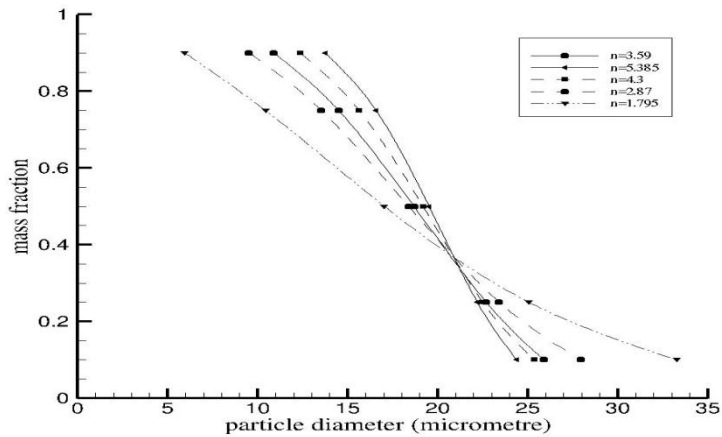


Figure 3.14: Various Particle Size Distribution

Fig.3.15 shows the particle velocity in outlet by using various size distribution of particles. If the size distribution parameter ‘n’ is decreased, then the particle distribution have smaller particles as well as larger particles but the smaller particles have larger in number, this is the reason for increasing the mean velocity of particles in the outlet. If the parameter ‘n’ is increased, the particle velocity in the outlet was decreased.

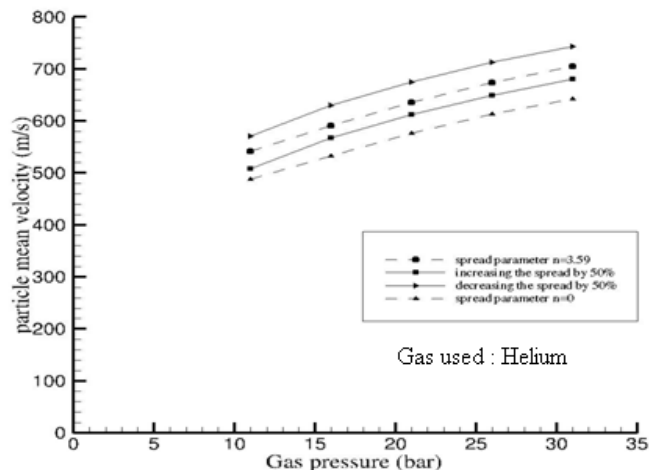


Figure 3.15: Effect Particle Size Distribution on Mean Particle Velocity

#### IV. Conclusion

The velocity of copper particles achieved in a cold spray nozzle were analysed with different particle size distributions, different gases, different gas pressure & temperature, one way & two way couplings and different turbulence models using CFD simulations. The simulation results showed that:

- The Mach number of the gas increases with a decrease in pressure along the axis of the nozzle. This results in greater gas velocity toward the nozzle exit.
- The results show that by increasing the gas temperature increases the gas velocity more significantly than the gas pressure, which shows that the gas velocity is a function of gas temperature and not the gas pressure.
- The results shows the particle size distribution plays a major role in the particle exit velocity i.e. lighter particles travels much faster than heavier particles.
- In the simulation argon, nitrogen and helium were used for spraying copper particles. Results show that helium is a far better carrier gas because particles achieve much higher velocity when helium is used for spraying.
- The temperature of the gas influences the velocity of copper particles because the density of gas decreases with increasing gas temperature and hence there is a greater gas velocity to accelerate the copper particles.
- Increasing the applied gas pressure increase the density of the gas which results in more drag on the particles. Increasing gas pressure does not affect the velocity of gas.
- The 2d analysis does not shows any difference between one way & two way coupling but the 3d analysis shows some difference in particle velocity.
- The turbulence analysis shows the turbulent activity is high at the starting time of the flow after that it will be reduced and the flow becomes stable.
- The turbulence analysis also shows the production of turbulent kinetic energy is high in area where large velocity gradient.

#### REFERENCES

- [1] Tobias Schmidt, Hamid Assadi, Frank Gartner, Horst Richter, Thorsten Stoltenhoff, Heinrich Kreye, and Thomas Klassen, From Particle Acceleration to Impact and Bonding in Cold Spraying, Journal of Thermal Spray Technology, JTTEE 18, 2009, p. 794-808
- [2] Tiziana Marrocco, Cold Spray Technology from TWI, TWI Technology Centre (Yorkshire), 2007
- [3] V.F. Kosarev, S.V. Klinkov, A.P. Alkhimov, and A.N. Papyrin, On some aspects of gas dynamic of the cold spray process, ASM international, 2003, JTTEE5 12:265-281
- [4] J. Karthikeyan, Cold spray technology: International status and USA efforts, ASB Industries, Inc., december 2004
- [5] P. Fauchais, A. Vardelle, and B. Dussoubs, Quo Vadis Thermal Spraying, ASM International, JTTEE 10, 2001, p. 44-66
- [6] C.-J. Li and A. Ohmori, Relationships Between the Microstructure and Properties of Thermally Sprayed Deposits, Journal of Thermal Spray Technology, JTTEE5 11, 2002, p. 365-374
- [7] Cast steel: Advances in Thermal Spray Technology, <http://www.keytometals.com/Articles/Art138.htm>, 2010, p. 1-2
- [8] Jin Kawakita a, Hiroshi Katanoda b, Makoto Watanabe a, Kensuke Yokoyama a, Seiji Kuroda a, Warm Spraying: An improved spray process to deposit novel coatings, Surface & Coating Technology, 202, 2008, p. 4369-4373
- [9] Thermal spray products, file:///F:/27April/thermalsprayprocesses.html, Metallisation
- [10] J. Karthikeyan, Evolution of cold spray technology, <http://www.entrepreneur.com/tradejournals/article/print/146546589.html>, 2010
- [11] G. D. Davis\*, G. B. Groff, R. A. Zatorski, Plasma Spray Coatings as Treatments for Aluminum, Titanium and Steel Adherends, Surface and Interface Analysis, VOL. 25, 1997, p. 366-373
- [12] Rainer Gadow, Andreas Killinger, and Johannes Rauch, Introduction to High-Velocity Suspension Flame Spraying (HVSFS), Journal of Thermal Spray Technology, JTTEE5 17, 2008, p. 655-661
- [13] Mingheng Li, Panagiotis D. Christofides, Multi-scale modelling and analysis of an industrial HVOF thermal spray process, Journal of chemical Engineering Science, 60, 2005, p. 3649-3669.
- [14] J. Rauch, G. Bolelli, A. Killinger, R. Gadow, V. Cannillo, L. Lusvarghi, Advances in High Velocity Suspension Flame Spraying (HVSFS), Journal of thermal spray technology, JTTEE 15, 203, 2009, 2131-2138
- [15] Sergei Vladimirovich Klinkov, Vladimir Fedorovich Kosarev, Martin Rein, Cold spray deposition: Significance of particle impact phenomena, Journal of Thermal spray technology, JTTEE, 9, 2005, p. 582-591
- [16] Anatolii Papyrin, Vladimir Kosarev, Sergey Klinkov, Anatolii Alkhimov, Vasily Fomin, Cold Spray Technology, JTTEE 12, 2007
- [17] F. Gärtner, T. Schmidt, T. Stoltenhoff and H. Kreye, Recent Developments and Potential Applications of Cold Spraying, Wiley Inter Science, 8 no.7, 2006, 611-618
- [18] Frank Gaertner, Tobias Schmidt, Heinrich Kreye, Present Status and Future Prospects of Cold Spraying, Trans Tech Publications, Switzerland, vols. 534-536, 2007, p. 433-436
- [19] R.E. Blose, B.H. Walker, R.M. Walker, S.H. Jroes, New opportunities to use cold spray process for applying additive features to titanium alloys, ASME, 2006, p. 30-37



- [20] Vladimir F. Kosarev\*, Sergey V. Klinkov and Aleksey A. Sova, Recently Patented Facilities and Applications in Cold Spray Engineering, BenthamScience Publishers Ltd, 2007, p. 35-42
- [21] T. Stoltenhoff, H. Kreye, and H.J. Richter, An Analysis of the Cold Spray Process and Its Coatings, Journal of Thermal Spray Technology, JTTEE511, 2002, p. 542-550
- [22] T. Han, B.A. Gillispie, and Z.B. Zhao, An Investigation on Powder Injection in the High-Pressure Cold Spray Process, Journal of Thermal Spray Technology, JTTEE5 18, 2009, p. 320-330
- [23] Saden H. Zahiri, William Yang, and MahnazJahedi, Characterization of cold spray titanium supersonic jet, Journal of Thermal Spray Technology, JTTEE5 18, 2009, 110-117
- [24] Wen-Ya Li and Chang-Jiu Li, Optimal design of a novel cold spray gun nozzle at a limited space, Journal of Thermal Spray Technology, JTTEE514, 2005, 391-396
- [25] T. Schmidt, F. Gaertner, and H. Kreye, New Development in Cold Spray Based on Higher Gas and Particle Temperature, Journal of Thermal Spray Technology, JTTEE5 15, 2006, 488-494
- [26] M Grujicic, W S DeRosset and D Helfritsch, Flow analysis and nozzle shape optimization for the cold-gas dynamic-spray process, ProQuest Science Journals, 217 part B, 2003, p. 1603-1613
- [27] M. Fukumoto, M. Mashiko, M. Yamada, and E. Yamaguchi, Deposition Behavior of Copper Fine Particles onto Flat Substrate Surface in Cold Spraying, Journal of Thermal Spray Technology, JTTEE5 19, 2010, 89-94
- [28] T. Van Steenkiste and J.R. Smith, Evaluation of Coatings Produced via Kinetic and Cold Spray Processes, Journal of Thermal Spray Technology, JTTEE5 13, 2004, p. 274-282
- [29] Victor K. Champagne, The Repair of Magnesium Rotorcraft Components by Cold Spray, ASME, 2008, p. 164-175
- [30] V. Shukla, G.S. Elliott, and B.H. Kear, Nanopowder Deposition by Supersonic Rectangular Jet Impingement, Journal of Thermal Spray Technology, JTTEE 59, 2000, p. 394-398
- [31] J.G. Legoux, E. Irissou, and C. Moreau, Effect of Substrate Temperature on the Formation Mechanism of Cold-Sprayed Aluminum, Zinc and Tin Coatings, Journal of Thermal Spray Technology, JTTEE5 16, 2007, p.619-627
- [32] X. Luo · G. Wang · H. Olivier, Parametric investigation of particle acceleration in high enthalpy conical nozzle flows for coating applications, ASME, 2008, 351-362
- [33] John D. Anderson, Modern Compressible Flow, Third Edition, McGraw- Hill Companies, Inc., p. 228-229
- [34] C. S. JOG, Fluid Dynamics, Second Edition, volume-2, Alpha Science International Ltd., p. 412-414
- [35] B. Jodoin, Cold Spray Nozzle Mach Number Limitation, Journal of Thermal Spray Technology, JTTEE5 11, 2002, p. 496-507
- [36] Cold spray, file://E:\mass flow rate\mm\_mp\_ct\_cs.html, Applied Research Laboratory at Penn State, 2010, p. 1-4
- [37] M. Grujicic, J.R. Saylor, D.E. Beasley, W.S. DeRosset, D. Helfritsch, Computational analysis of the interfacial bonding between feed-powder particles and the substrate in the cold-gas dynamic-spray process, JTTEE 41, 219, 200, p. 211-227
- [38] R. Morgan\*, P. Fox, J. Pattison, C. Sutcliffe, W. O'Neill, Analysis of cold gas dynamically sprayed aluminium deposits, ASME, 58, 2004, p. 1317-1320
- [39] Wen-Ya Li \*, Hanlin Liao, G. Douchy, C. Coddet, Optimal design of a cold spray nozzle by numerical analysis of particle velocity and experimental validation with 316L stainless steel powder, Journal of thermal spray technology, JTTEE 7, 2007, p. 2129-2137
- [40] Introduction to Fluent Inc., Chapter 2, 2006, 2-(1-2)
- [41] B. Samareh, A. Dolatabadi, A Three-Dimensional Analysis of the Cold Spray Process: Effect of Substrate Location and Shape, Concordia University, Montreal
- [42] Y. Li, A. Kirkpatrick, C. Mitchell, B. Willson, Characteristics and Computational Fluid Dynamics Modelling of High-Pressure Gas Jet Injection, ASME, vol. 126, January 2004, p. 192-198
- [43] R.Lupoi, W.O'Neill, Powder stream characteristics in cold spray nozzles, Surface and Coatings Technology, 206(2011), p. 1069-1076.
- [44] D.L.Gilmore, R.C.Dykhuzen, R.A.Neiser, T.J.Roemer, and M.F.Smith, Particle velocity and deposition efficiency in the cold spray process, JTTEE5:576-582